

# THE SOLUTION OF THE NEUTRON DIFFUSION EQUATION BY THE HIERARCHICAL EXPANSION METHOD

Eduardo Lobo Lustosa Cabral

IPEN-CNEN/SP

RAS - Departamento de Reatores  
Travessa R, 400 - Cidade Universitária  
05508-900 São Paulo, SP  
e-mail: elcabral@net.ipen.br

## ABSTRACT

A nodal method for the numerical solution of the two-dimensional two-group neutron diffusion equation in rectangular geometry is presented. The method is based on the expansion of the group neutron fluxes by hierarchical functions. The weighted residual procedure is used to obtain the solution equations. The expansion functions are Legendre polynomials adjusted in the rectangular nodes in a novel form, so that corner, side and surface functions are distinguished. The order of the approximation for the side and surface expansion functions are up to desired or necessary degree. This formalism has been programmed in a computer code called HEMDC. The two-dimensional IAEA benchmark problem was tested, showing the capability of the method to yield accurate numerical solutions on coarse spatial grids.

## INTRODUCTION

Nodal methods have been developed to generate accurate, fast answers to the unknown behavior of the neutron flux within nuclear reactor cores, i.e., the solution of the 2D or 3D space-time transport or diffusion equations, extended over the whole core domain. Although it is possible to simplify the nuclear reactor core, by considering that it is composed of a number of large subdomains (nodes) with homogenized neutronic properties, the solution is yet a quite expensive task, specially in 3D and/or dynamic problems, because of the large number of variables involved.

In this paper, we present a new nodal method to solve numerically the neutron diffusion equation. The method is based on an expansion of the group neutron fluxes in hierarchical polynomials associated with the weighted-residual classical formulation (Galerkin) to derive the discretized equations. The static two-energy group diffusion equation and a 2D rectangular mesh are used to show the applicability of the method. This method is similar to the nodal methods where a coarse mesh is used, but it is a one level method that does not require coupling coefficients at the nodal interfaces.

## TWO GROUP NEUTRON DIFFUSION EQUATION AND THE WEIGHTED RESIDUAL METHOD

The static energy group neutron diffusion equation

can be written in general form as:

$$-D_g \nabla^2 \phi_g + \Sigma_g \phi_g = F_g, \quad (1)$$

where conventional notations have been used, external neutron sources have not been considered, the subscript  $g$  is either 1 or 2 referring to the fast and to the thermal neutron flux respectively, and  $F_g$  is the fission source for the fast energy group and the downscattering source for the thermal energy group. The boundary conditions can be written in general form as,

$$D_g \vec{\nabla} \phi_g \cdot \vec{n} + b \phi_g = 0, \quad (2)$$

where  $\vec{n}$  is the unit vector normal to the boundary pointing outward to the surface, and  $b$  is a constant. Equation. (2) allows to represent the most commonly used boundary conditions in diffusion theory.

To apply the weighted residual method, the solution domain, i.e., the reactor is partitioned into regions  $\Omega$ . The regions in this work are rectangles, and each region is assumed to be homogeneous, i.e., the material properties are constant. The assumption of homogeneous regions is not imposed by the method, but it is assumed here for simplicity, and in practice, this is almost always the case. The fast and thermal neutron fluxes in each region are approximated by linear combination of basis functions as follows:

$$\phi_g = \sum_{m=1}^M a_{g,m} P_m(\xi, \eta), \quad (3)$$

where  $P_m$  is the  $m^{\text{th}}$  expansion function,  $a_{g,m}$  is a coefficient corresponding to the  $m^{\text{th}}$  expansion function,  $M$  is the number of functions used to approximate the fluxes, and  $\xi$  and  $\eta$  are the local coordinates of the region. The expansion functions are special polynomials, that we describe in the next section. The local coordinates are related to the  $x$  and  $y$  coordinates of the whole domain by the expressions

$$\xi = 2 \frac{(x - x_{i,j})}{\Delta x_{i,j}}, \quad \eta = 2 \frac{(y - y_{i,j})}{\Delta y_{i,j}}, \quad (4)$$

where the  $x_{i,j}$  and  $y_{i,j}$  are the coordinates of the center of region  $i,j$ . Moreover,  $\Delta x_{i,j}$  and  $\Delta y_{i,j}$  are the region-edge lengths in the  $x$  and  $y$  directions respectively.

As with the weighted residual procedure, the coefficients  $a_m$  are the solutions of a system of equations obtained by weighting and integrating the balance equations over the regions of the domain. The functions used as weight, in the classical Galerkin method and in this work, are the same as the expansion functions. Applying the weighted residual procedure in Eq. (1) subject to the boundary conditions given by Eq. (2), we obtain:

$$-\int_{\Omega} P_m D_g \nabla^2 \phi_g d\Omega + \int_{\Omega} P_m \Sigma_g \phi_g d\Omega + \int_{\Gamma} P_m (D_g \bar{\nabla} \phi_g \cdot \bar{n} + b \phi_g) d\Gamma = \int_{\Omega} P_m F_g d\Omega, \quad m = 1, \dots, M, \quad (5)$$

where  $\Gamma$  is the boundary of the domain. We remark that the third term is presented only for the regions at the reactor boundary. This equation represents a system of  $M$  equations for each region. Substituting Eq. (3) into Eq. (5) and applying the Green's Theorem to the first term, we obtain:

$$D_g^{i,j} \sum_{n=1}^M a_{g,n}^{i,j} \int_{\Omega} (\bar{\nabla} P_m \cdot \bar{\nabla} P_n) d\Omega - \sum_{n=1}^M a_{g,n}^{i,j} \int_{\Omega} (P_m P_n) d\Omega + b \sum_{n=1}^M a_{g,n}^{i,j} \int_{\Gamma} (P_m P_n) d\Gamma = \sum_{n=1}^M f_{g,n}^{i,j} \int_{\Omega} (P_m P_n) d\Omega, \quad m = 1, \dots, M. \quad (6)$$

Here the superscripts  $i$  and  $j$  refers to node  $i,j$  and  $f_{g,n}$  represents the source coefficients. These coefficients are not new unknowns but algebraic combinations of the fast and thermal fluxes coefficients and material properties. Now, changing the space coordinates from the global coordinate system,  $x$  and  $y$ , to the local coordinate system,  $\xi$  and  $\eta$ , using Eq. (4), we write the resulting equation in matrix form

$$\underline{A}_g^{i,j} \bar{a}_g^{i,j} = \bar{f}_g^{i,j}, \quad (7)$$

where  $\bar{a}_g^{i,j}$  is an  $M$ -dimensional vector containing the coefficients  $a_{g,m}$  for node  $i,j$ ,  $\bar{f}_g^{i,j}$  is an  $M$ -dimensional vector formed by the group source for node  $i,j$ , and  $\underline{A}_g^{i,j}$  is a  $M \times M$  nodal matrix, whose element  $m,n$  is given by

$$\begin{aligned} A_{g,m,n}^{i,j} = & 4D_g^{i,j} \left[ \frac{1}{\Delta x_{i,j}^2} \int_{-1}^1 \int_{-1}^1 \left( \frac{\partial P_m}{\partial \xi} \frac{\partial P_n}{\partial \xi} \right) d\xi d\eta + \right. \\ & \left. + \frac{1}{\Delta y_{i,j}^2} \int_{-1}^1 \int_{-1}^1 \left( \frac{\partial P_m}{\partial \eta} \frac{\partial P_n}{\partial \eta} \right) d\xi d\eta \right] + \Sigma_g^{i,j} \int_{-1}^1 \int_{-1}^1 (P_m P_n) d\xi d\eta + \\ & + b \int_{-1}^1 [P_m P_n]_{\xi=1} d\eta + b \int_{-1}^1 [P_m P_n]_{\eta=1} d\xi. \end{aligned} \quad (8)$$

The last two terms of the right hand side appear only for the nodes at the reactor boundaries. The reactor boundary is represented here, as an example, located at coordinates  $\xi = 1$  and  $\eta = 1$ . The  $m^{\text{th}}$  component of the source vector  $\bar{f}_g^{i,j}$  for node  $i,j$  for the fast flux is given by

$$f_{1,m}^{i,j} = \frac{1}{\lambda} \sum_{n=1}^M \left( v_1 \Sigma_{f1}^{i,j} a_{1,n}^{i,j} + v_2 \Sigma_{f2}^{i,j} a_{2,n}^{i,j} \right) \int_{-1}^1 \int_{-1}^1 P_m P_n d\xi d\eta \quad (9)$$

and, for the thermal flux by

$$f_{2,m}^{i,j} = \Sigma_{f2}^{i,j} \sum_{n=1}^M \left( a_{1,n}^{i,j} \int_{-1}^1 \int_{-1}^1 P_m P_n d\xi d\eta \right). \quad (10)$$

Equation (7) represents the neutron balance equation for energy group  $g$  for a single node. However, more than one node share the same coefficients  $a_{g,m}$ , as we describe in the following sections.

## HIERARCHICAL FUNCTIONS

In the finite element method the coefficients  $a_{g,m}$  are identified with the fluxes at specified locations. This identification has been widely followed in the finite element literature and has the merit of assigning a "physical" meaning to the parameters  $a_{g,m}$ . There is, however, a disadvantage in this definition, that becomes apparent when the shape functions for linear, quadratic, and cubic polynomials, for the one dimensional case, and the resulting nodal matrices are examined.

Figure 1 shows a typical node assignment for the standard shape functions. With the nodes equally spaced within the region, the shape functions are normally the following:

Linear:

$$P_0 = -\frac{\xi-1}{2}, \quad P_1 = \frac{\xi+1}{2} \quad (11)$$

Quadratic:

$$P_0 = -\frac{\xi(\xi-1)}{2}, \quad P_1 = -(\xi-1)(\xi+1),$$

$$P_2 = \frac{\xi+1}{2} \quad (12)$$

Cubic:

$$P_0 = -\frac{9}{16}(\xi + \frac{1}{3})(\xi - \frac{1}{3})(\xi - 1); \quad P_1 = \frac{27}{16}(\xi + 1)(\xi - \frac{1}{3})(\xi - 1);$$

$$P_2 = -\frac{27}{16}(\xi + 1)(\xi + \frac{1}{3})(\xi - 1); \quad P_3 = \frac{9}{16}(\xi + 1)(\xi + \frac{1}{3})(\xi - \frac{1}{3}). \quad (13)$$

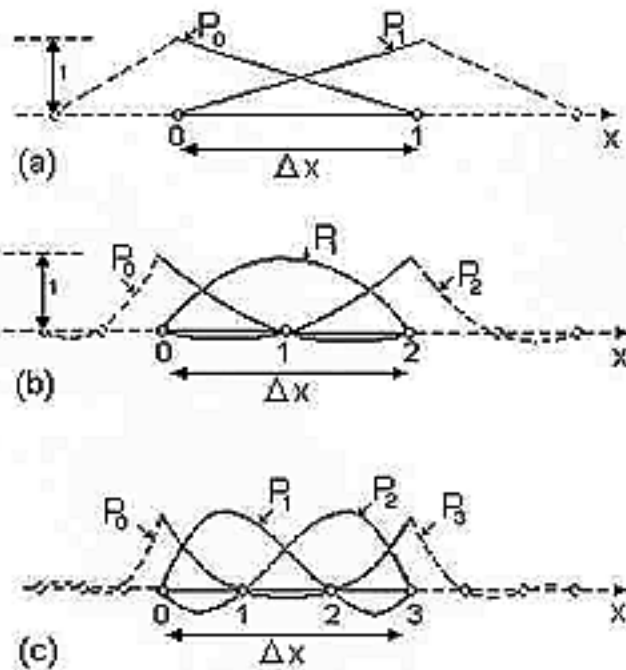


Figure 1. One-Dimensional Elements and Associated Standard Shape Functions of (a) Linear, (b) Quadratic, and (c) Cubic Form. See ref. [1].

For these polynomial functions, the nodal matrix  $\underline{A}_g^{i,j}$ , considering just the  $\xi$  direction in the coefficients given by Eq. (8), for linear, quadratic, and cubic elements are the following:

Linear:

$$\underline{A}_g^{i,j} = \begin{bmatrix} \frac{D_g^{i,j}}{\Delta x_{i,j}^2} + \frac{\Sigma_g^{i,j}}{3} & -\frac{D_g^{i,j}}{\Delta x_{i,j}^2} + \frac{\Sigma_g^{i,j}}{6} \\ -\frac{D_g^{i,j}}{\Delta x_{i,j}^2} + \frac{\Sigma_g^{i,j}}{6} & \frac{D_g^{i,j}}{\Delta x_{i,j}^2} + \frac{\Sigma_g^{i,j}}{3} \end{bmatrix} \quad (14)$$

Quadratic:

$$\underline{A}_g^{i,j} = \begin{bmatrix} \frac{7D_g^{i,j}}{3\Delta x_{i,j}^2} + \frac{2\Sigma_g^{i,j}}{15} & -\frac{8D_g^{i,j}}{3\Delta x_{i,j}^2} + \frac{\Sigma_g^{i,j}}{15} & \frac{D_g^{i,j}}{3\Delta x_{i,j}^2} - \frac{\Sigma_g^{i,j}}{30} \\ \frac{8D_g^{i,j}}{3\Delta x_{i,j}^2} + \frac{\Sigma_g^{i,j}}{15} & \frac{16D_g^{i,j}}{3\Delta x_{i,j}^2} + \frac{8\Sigma_g^{i,j}}{15} & \frac{8D_g^{i,j}}{3\Delta x_{i,j}^2} + \frac{\Sigma_g^{i,j}}{15} \\ \frac{D_g^{i,j}}{3\Delta x_{i,j}^2} - \frac{\Sigma_g^{i,j}}{30} & -\frac{8D_g^{i,j}}{3\Delta x_{i,j}^2} + \frac{\Sigma_g^{i,j}}{15} & \frac{7D_g^{i,j}}{3\Delta x_{i,j}^2} + \frac{2\Sigma_g^{i,j}}{15} \end{bmatrix} \quad (15)$$

Cubic:

$$\underline{A}_g^{i,j} = \begin{bmatrix} \frac{37D_g^{i,j}}{10\Delta x_{i,j}^2} + \frac{8\Sigma_g^{i,j}}{105} & \frac{189D_g^{i,j}}{40\Delta x_{i,j}^2} + \frac{33\Sigma_g^{i,j}}{560} & \frac{27D_g^{i,j}}{20\Delta x_{i,j}^2} - \frac{\Sigma_g^{i,j}}{140} & \frac{13D_g^{i,j}}{40\Delta x_{i,j}^2} + \frac{19\Sigma_g^{i,j}}{1680} \\ \frac{189D_g^{i,j}}{40\Delta x_{i,j}^2} + \frac{33\Sigma_g^{i,j}}{560} & \frac{54D_g^{i,j}}{5\Delta x_{i,j}^2} + \frac{27\Sigma_g^{i,j}}{70} & \frac{297D_g^{i,j}}{40\Delta x_{i,j}^2} + \frac{27\Sigma_g^{i,j}}{560} & \frac{27D_g^{i,j}}{20\Delta x_{i,j}^2} - \frac{\Sigma_g^{i,j}}{140} \\ \frac{27D_g^{i,j}}{20\Delta x_{i,j}^2} - \frac{\Sigma_g^{i,j}}{140} & \frac{297D_g^{i,j}}{40\Delta x_{i,j}^2} + \frac{27\Sigma_g^{i,j}}{560} & \frac{54D_g^{i,j}}{5\Delta x_{i,j}^2} + \frac{27\Sigma_g^{i,j}}{70} & \frac{189D_g^{i,j}}{40\Delta x_{i,j}^2} + \frac{33\Sigma_g^{i,j}}{560} \\ \frac{13D_g^{i,j}}{40\Delta x_{i,j}^2} + \frac{19\Sigma_g^{i,j}}{1680} & \frac{27D_g^{i,j}}{20\Delta x_{i,j}^2} - \frac{\Sigma_g^{i,j}}{140} & \frac{297D_g^{i,j}}{40\Delta x_{i,j}^2} + \frac{27\Sigma_g^{i,j}}{560} & \frac{37D_g^{i,j}}{10\Delta x_{i,j}^2} + \frac{8\Sigma_g^{i,j}}{105} \end{bmatrix} \quad (16)$$

As the nodal matrix in the above equations for each order of approximation are completely different, each level of approximation results in a completely new nodal matrix, and thus, the equation set has to be entirely reevaluated if it is decided to resolve a problem using shape functions of a higher degree. This type of approximation contrasts sharply with the continuous function approximation given by Eq. (3), in which when the solution is refined by increasing the total number  $M$  of the expansion functions used, the form of the lower order expansion functions remained unaltered. In this approach the expansion functions represent simply additive refinements of higher order. Such expansion functions are called hierarchical, as their contribution to the approximation will be of less importance as the order increases.

Further, if the chosen expansion functions are orthogonal, the nodal matrices obtained at each stage of refinement ensure a better conditioning of the system of equations to be solved and show a diagonal structure. Although complete diagonality of the approximation is impossible to achieve, it must be attempted to achieve as weak a coupling as possible between the various levels of approximation. In the problem of neutron diffusion the predominant terms in the nodal matrix are the diffusion terms, that have the following general form:

$$D_g \int_{\Omega} \frac{\partial P_m}{\partial \xi} \frac{\partial P_n}{\partial \xi} d\Omega. \quad (17)$$

If the expansion function sets, containing the appropriate polynomials, can be found for which such integrals are zero for  $m \neq n$ , then orthogonality is almost achieved.

Clearly, the linear expansion over a one dimensional element can only be given by the shape function of Eq. (11) and cannot be improved. However, hierarchical form can be achieved over this element if higher order polynomials are used to modify this linear expansion. One set of

polynomial functions which has orthogonality property, with respect to Eq. (17) over the range  $-1 \leq \xi \leq 1$ , is the set of Legendre polynomials  $P_m(\xi)$ . As an example, Legendre polynomials of degree 2, 3, 4 and 5, are given by [1]

$$\begin{aligned} P_2 &= \xi^2 - 1, & P_4 &= \frac{1}{4}(15\xi^4 - 18\xi^2 + 3), \\ P_3 &= 2(\xi^3 - \xi), & P_5 &= 7\xi^5 - 10\xi^3 + 3\xi. \end{aligned} \quad (18)$$

A plot of these functions, up to the third degree, is given in Fig. 2.

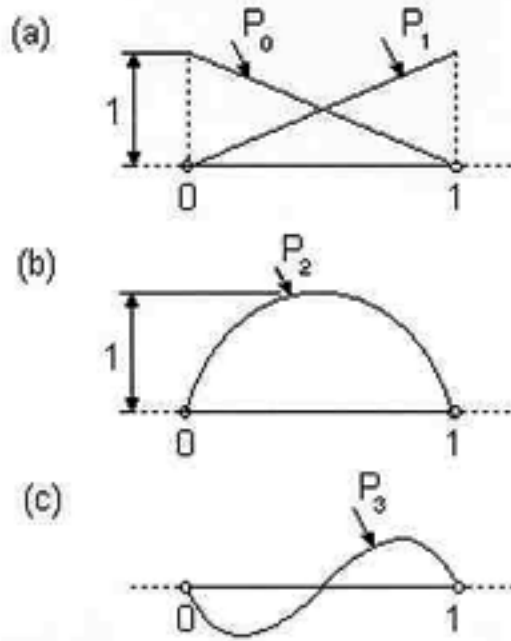


Figure 2. Hierarchical Element Shape Functions of Nearly Orthogonal Form, (a) Linear, (b) Quadratic, and (c) Cubic.

For these polynomials the nodal matrix  $\underline{A}_g^{i,j}$ , considering just the  $\xi$  direction in the coefficients given by Eq. (8), for linear, quadratic, and cubic elements appear as

Linear:

$$\underline{A}_g^{i,j} = \begin{bmatrix} \frac{D_g^{i,j}}{\Delta x_{i,j}^2} + \frac{\Sigma_g^{i,j}}{3} & -\frac{D_g^{i,j}}{\Delta x_{i,j}^2} + \frac{\Sigma_g^{i,j}}{6} \\ \frac{D_g^{i,j}}{\Delta x_{i,j}^2} + \frac{\Sigma_g^{i,j}}{6} & -\frac{D_g^{i,j}}{\Delta x_{i,j}^2} + \frac{\Sigma_g^{i,j}}{3} \end{bmatrix} \quad (19)$$

Quadratic:

$$\underline{A}_g^{i,j} = \begin{bmatrix} \frac{D_g^{i,j}}{\Delta x_{i,j}^2} + \frac{\Sigma_g^{i,j}}{3} & -\frac{D_g^{i,j}}{\Delta x_{i,j}^2} + \frac{\Sigma_g^{i,j}}{6} & -\frac{\Sigma_g^{i,j}}{3} \\ \frac{D_g^{i,j}}{\Delta x_{i,j}^2} + \frac{\Sigma_g^{i,j}}{6} & -\frac{D_g^{i,j}}{\Delta x_{i,j}^2} + \frac{\Sigma_g^{i,j}}{3} & \frac{\Sigma_g^{i,j}}{3} \\ -\frac{\Sigma_g^{i,j}}{3} & \frac{\Sigma_g^{i,j}}{3} & \frac{16D_g^{i,j}}{3\Delta x_{i,j}^2} + \frac{8\Sigma_g^{i,j}}{15} \end{bmatrix} \quad (20)$$

Cubic:

$$\underline{A}_g^{i,j} = \begin{bmatrix} \frac{D_g^{i,j}}{\Delta x_{i,j}^2} + \frac{\Sigma_g^{i,j}}{3} & -\frac{D_g^{i,j}}{\Delta x_{i,j}^2} + \frac{\Sigma_g^{i,j}}{6} & -\frac{\Sigma_g^{i,j}}{3} & \frac{2\Sigma_g^{i,j}}{15} \\ \frac{D_g^{i,j}}{\Delta x_{i,j}^2} + \frac{\Sigma_g^{i,j}}{6} & -\frac{D_g^{i,j}}{\Delta x_{i,j}^2} + \frac{\Sigma_g^{i,j}}{3} & \frac{\Sigma_g^{i,j}}{3} & -\frac{2\Sigma_g^{i,j}}{15} \\ -\frac{\Sigma_g^{i,j}}{3} & \frac{\Sigma_g^{i,j}}{3} & \frac{16D_g^{i,j}}{3\Delta x_{i,j}^2} + \frac{8\Sigma_g^{i,j}}{15} & 0 \\ \frac{2\Sigma_g^{i,j}}{15} & -\frac{2\Sigma_g^{i,j}}{15} & 0 & \frac{164D_g^{i,j}}{5\Delta x_{i,j}^2} + \frac{32\Sigma_g^{i,j}}{105} \end{bmatrix} \quad (21)$$

In each step, we can see that as the approximation is refined, the matrices produced by the previous stage of approximation reoccur and need not be recomputed. Obviously absolute orthogonality is not achieved but it is easily observed that the terms of the main diagonal are predominant over the other entries.

## TWO DIMENSIONAL RECTANGULAR HIERARCHICAL SHAPE FUNCTIONS

With the one-dimensional hierarchical expansion functions already established, the generation of hierarchical expansion functions for rectangular two-dimensional elements is trivial. Any product of a one-dimensional hierarchical shape function in the local element variable along the edge, say  $\xi$ , with a linear (or hierarchical) function in the other local element direction,  $\eta$ , proves to be acceptable, and polynomial terms (of any degree) can be obtained by forming such simple products. Using the one-dimensional functions of Eq. (18), the expansion functions for the element shown in Fig. 3 can be written as follows.

Typical corner node (3):

$$P_3(\xi, \eta) = \frac{1}{4}(1+\eta)(1-\xi). \quad (22)$$

Typical side (2-3):

$$P_{2(2-3)}(\xi, \eta) = \frac{1}{2}(1+\eta)(\xi^2 - 1), \quad (23)$$

$$P_{3(2-3)}(\xi, \eta) = \frac{1}{6}(1+\eta)(\xi^3 - \xi). \quad (24)$$

Observe that the value of  $P_3$  is zero in the corners 0, 1 and 2, and also that, the functions  $P_{2(2-3)}$  and  $P_{3(2-3)}$  are zero in all corners, and in the other three sides.

Expansion functions to improve the solution inside a single node can be obtained by the product of two functions of degree greater than two in both directions. For instance,

$$P_{2(\text{area})}(\xi, \eta) = \frac{1}{4}(\xi^2 - 1)(\eta^2 - 1), \quad (25)$$

provides a suitable expansion function, which will be associated with a parameter that is not connected between

nodes, i.e., a parameter that is internal to a single node. This parameter can be thought of as representing the nodal area. Observe that the value of this function is zero in the four corners and in the four sides of the node.

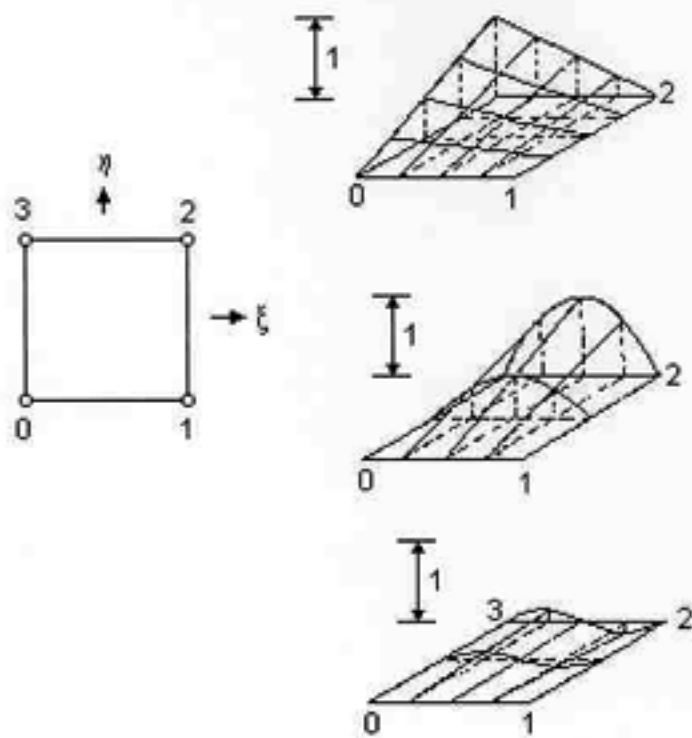


Figure 3. Hierarchical Element Expansion Functions on a Rectangular Node.

The numbering of nodal and hierarchical parameters in a logical sequence presents an interesting problem, as the label corresponding to a hierarchical degree of freedom can be associated either with a corner or an element side or with a single element. Figure 4 shows a node with the parameters associated with its corners, sides, and area.  $\phi_{i,j}$  are the corner parameters associated with the linear expansion functions,  $a_{i,j,m}^x$  and  $a_{i,j,m}^y$  are the side parameters associated with the side expansion functions, and  $a_{i,j,m}^A$  are the area parameters associated with the area expansion functions. The order of the approximation for the side and area expansion functions are up to desired or necessary degree.

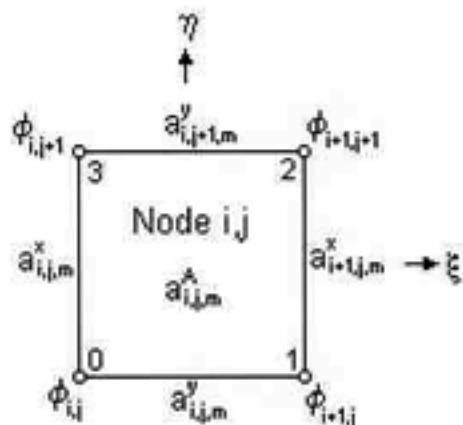


Figure 4. Two-Dimensional Rectangular Node and Its Associated Parameters.

Futhermore, it should be observed that it is very easy to add polynomial expansions locally to achieve a refinement in the region where the neutron fluxes varies

most rapidly and where the approximation is therefore prone to the largest errors.

Observe that the corner parameters are physically associated with the group flux at the corner points. The parameter  $\phi_{i,j}$  is associated with expansion function  $P_0$  in node  $i,j$ . Also, this same parameter is associated with function  $P_1$  in node  $i,j-1$ , with function  $P_2$  in node  $i-1,j-1$ , and with function  $P_3$  in node  $i-1,j$ . Thus, the corner parameters are connected to four different nodes through four different expansion functions. The side parameters  $a_{i,j,m}^x$  and  $a_{i,j,m}^y$  are connected with two nodes. The area parameters are connected with a single node. Therefore, the hierarchical variables associated with any corner or side with the same value on the adjacent elements will automatically guarantee the uniqueness and continuity of the fluxes at the element boundaries.

As mentioned earlier, Eq. (7) represents the neutron balance for energy group  $g$  for a single node, and as observed, the corner and side parameters are shared by more than a single node. Therefore, before the coefficients can be calculated, there must be an assembly process to add up the contributions from the nodal matrices into the global system matrices. The assembly of the nodal matrices into the global system matrices results in a homogeneous system of equations whose solution is a classical eigenvalue problem.

## NUMERICAL RESULTS

The method presented in the previous sections was implemented in the HEMDC computer code. The procedure used to calculate the coefficients  $a_{g,m}$  is the normally used in neutronic codes. The scheme consists of inner and outer iterations. In the inner iterations, the source is fixed and the Gauss-Siedel method is used to solve the system of equations. The outer iteration step is used to update the source given an estimate of the dominant solution, obtained from the inner iteration step. The method of Chebyshev Polynomials, applied to the coefficients  $a_{g,m}$ , is used to accelerate the convergence of the dominant solution.

In this paper, the 2D International Atomic Energy Agency (IAEA) Benchmark Problem have been calculated and related to other results reported. This problem is a 2D simplified four-zone LWR, consisting of 177, 20 cm X 20 cm fuel assemblies, and reflected radially and axially by 20 cm of water [2].

Three numerical solutions generated by HEMDC code for an octant with square mesh of 20 cm and 10 cm are given. For the 20 cm mesh 3<sup>rd</sup> and 5<sup>th</sup> order polynomial expansion are used. For the 10 cm mesh only a 3<sup>rd</sup> order expansion is performed. Table 1 presents the  $k$ -effective for the three solutions together with results from other codes, obtained from [2].

For illustration, Fig. 5 shows the HEMDC solution for the thermal flux distribution for the main diagonal (line  $y = x$ ). Figure 6 shows the thermal flux relative deviation

for the three solutions with respect to the results of the code MEDIUM-2 with a mesh size of 3 1/3 cm [3].

TABLE 1. Results of k-Effective From Several Codes and Conditions

Code	(mesh size, order)	K-effective
HEMDC	20 cm, 3 <sup>rd</sup>	1.029606
HEMDC	20 cm, 5 <sup>th</sup>	1.029553
HEMDC	10 cm, 3 <sup>rd</sup>	1.029582
MEDIUM-2 [3]	3 1/3 cm	1.029585
MEDIUM-2 [3]	10 cm	1.029611
FEMB [4]	4.7 cm, 2 <sup>nd</sup>	1.0296
FERM [5]	-	1.02961
VENTURE [6]	Extrapolated	1.02959

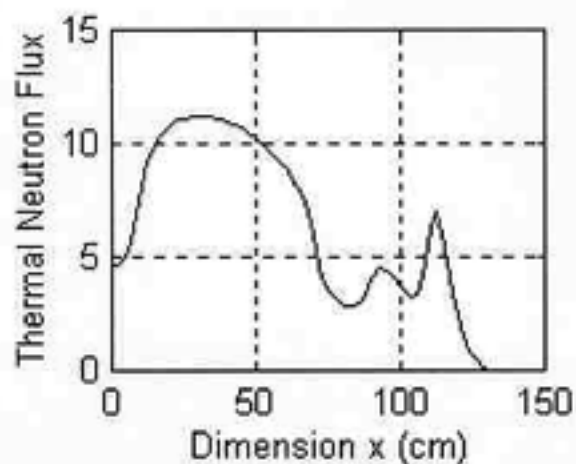


Figure 5. Thermal Neutron Flux at the Main Diagonal (Line  $y=x$ )

From Fig. 6 we observe that the relative deviation between the local fluxes calculated from the codes HEMDC and MEDIUM-2 are very small, less than 5% for the solution with a mesh of 10 cm and 3rd order expansion.

The CPU time used for the code HEMDC is not compared with other codes in this work, because no attempt was made to develop a computational efficient code, only the method has been evaluated.

## CONCLUSIONS

A nodal method for the solution of the two-dimensional two-group neutron diffusion equation in rectangular geometry has been developed and numerically evaluated. The method is based on the expansion of the group neutron fluxes by Legendre polynomials. The polynomials are adjusted in the rectangular nodes in a new form, so that corner, side and surface functions are distinguished. The order of the approximation for the side and surface expansion functions are up to desired or necessary degree. Numerical results for the two-dimensional IAEA benchmark problem have shown high accuracy for very coarse-mesh.

The simplicity of the method and the versatility of

HEMDC enable the extension of the methodology to three-dimensional cases and to space-time diffusion applications, which are under development.

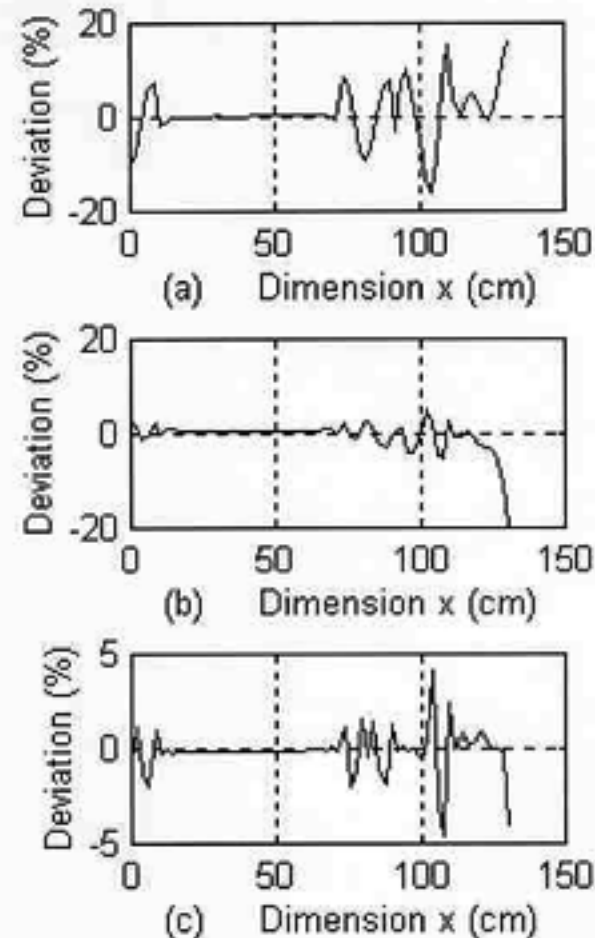


Figure 6. Relative Deviation in Percent of the Thermal Neutron Flux at  $y = x$ , for the Three Solutions; (a) 20 cm, 3<sup>rd</sup> Order; (b) 20 cm, 5<sup>th</sup> Order; and, (c) 10cm, 3<sup>rd</sup> Order.

## REFERENCES

- [1] Zienkiewicz, O.C., and Morgan, K., "Finite Elements and Approximation," John Wiley & Sons, New York, 1983.
- [2] "Benchmark Problem Book," ANL-7416 Suppl. II, Argonne National Laboratory, 1977.
- [3] Wagner, R.M. et al, "Validation of the Nodal Expansion Method and the Depletion Program MEDIUM-2 by Benchmark Calculations and Direct Comparison with Experiments," *Atomkernenergie*, Vol. 30, pp. 129, 1977.
- [4] Misfeldt, Ib, "Solution of the Multigroup neutron Diffusion Equations by the Finite Element Method," *Risø-M-1809*, 1975.
- [5] Nakata, H., and Martin, W.R., "The Finite Element Response Matrix Method," *Nucl. Sci. Eng.*, Vol. 85, pp. 289-305, 1983.
- [6] Vondy, D.R., Fowler, T.B., and Cunningham, G.W., "VENTURE: A Code Block for Solving Multigroup Neutronics Problems Applying the Finite-Difference Diffusion-Theory Approximation to Neutron Transport," *Technical Report ORNL-5062*, Oak Ridge National Laboratory, 1975.